

## The Effect of Variation of Corn Comb Fiber Composition on The Physical Properties of Biofoam with The Addition of Aerogel Silica

Tiara Widiastuti, Roniyus Marjunus\*, Agus Riyanto, and Dwi Asmi

Department of Physics, University of Lampung, Bandar Lampung, Indonesia, 35141

### Article Information

#### Article history:

Received February 8, 2023

Received in revised form

March 9, 2023

Accepted April 15, 2023

**Keywords:** biofoam, corn cob fiber, silica aerogel, physical test.

### Abstract

Styrofoam has many negative impacts because it harms health, pollutes the environment, and cannot decompose in nature. Efforts have been made to develop biofoam derived from natural kinds of stuff to reduce the harmful effects of styrofoam. So that they are safer and do not pollute the environment. Biofoam in this study was made from tapioca starch, corn cob fiber, a binding polymer in the form of Polyvinyl Alcohol (PVA), and a superhydrophobic agent in the form of silica aerogel. This research was conducted to determine the effect of variations in the composition of corn cob fiber on the physical properties of biofoam with the addition of silica aerogel. The production of corn cob fiber was carried out in two stages, namely using 10% NaOH to remove lignin and bleaching using 10% H<sub>2</sub>O<sub>2</sub> to bleach the fibers, which were then combined into the biofoam mixture. The production of biofoam used the thermopressing method with a temperature of 150° and pressed for 4 minutes with fiber variations of 13.75g, 16.25g, 18.75g, and 21.25g. Add conclusion of the research is 18.75 g of fiber with a water absorption value of (1.2 ± 0.2)%, a density of (0.5 ± 0.1)g/cm<sup>3</sup>, and a compressive strength of 3.60 MPa.

### Informasi Artikel

#### Proses artikel:

Diterima 8 Februari 2023

Diterima dan direvisi dari 9

Maret 2023

Accepted 15 April 2023

**Kata kunci:** biofoam, serat boggol jagung, silika aerogel, uji fisis.

### Abstrak

Styrofoam memiliki banyak dampak negatif karena dapat membahayakan kesehatan dan juga dapat mencemari lingkungan dan tidak bisa terurai di alam. Untuk mengurangi bahaya negatif dari styrofoam, saat ini telah dilakukan upaya pengembangan produk biofoam yang berasal dari bahan alami sehingga lebih aman dan tidak mencemari lingkungan. Biofoam pada penelitian ini terbuat dari pati tapioka, serat bonggol jagung, polimer pengikat berupa Polivinil Alkohol (PVA) dan agen superhidrofobik berupa silika aerogel. Penelitian ini dilakukan dengan tujuan untuk mengetahui pengaruh variasi komposisi serat bonggol jagung terhadap sifat fisis pada biofoam dengan penambahan silika aerogel. Pembuatan serat bonggol jagung ini dilakukan melalui dua tahap yaitu menggunakan NaOH 10% untuk menghilangkan lignin, dan bleaching menggunakan H<sub>2</sub>O<sub>2</sub> 10% untuk pemutihan pada serat yang kemudian digabungkan dalam adonan biofoam. Pembuatan biofoam menggunakan metode thermopressing dengan suhu 150° dan ditekan selama 4 menit dengan variasi serat 13,75g, 16,25g, 18,75g dan 21,25g. Hasil biofoam terbaik adalah dengan jumlah serat 18,75g dengan nilai daya serap air (1,2±0,2)%, densitas (0,5±0,1)g/cm<sup>3</sup>, dan kuat tekan 3,60MPa.

\*Corresponding author.

Email address: roniyus.1977@fmipa.unila.ac.id

## 1. Introduction

Food manufacturers widely use styrofoam as a packaging material for disposable food or beverage products, ready-to-eat, fresh, and ready-to-process food (Khalid et al., 2012). It is due to the advantages of styrofoam, which is not easy to leak, practical, lightweight, has an excellent ability to withstand heat and cold, and more economical (Sulchan & Endang, 2007). However, it turns out that styrofoam has many negative impacts because it can harm health and also can pollute the environment, and cannot be decomposed in nature (Khalid et al., 2012).

To reduce the harmful dangers of styrofoam have been made to develop biofoam products derived from natural materials so that they are safer and do not pollute the environment (Qiu et al., 2013). Biodegradable foam (biofoam) is an alternative packaging to replace styrofoam which uses the primary raw material in the form of starch so that the packaging can decompose naturally (Breuninger et al., 2009). Starch can be used as a raw material for making biodegradable plastic and biofoam. Starch is often used in the food industry as a biodegradable film to replace plastic polymers because it is economical, renewable, and provides good physical characteristics (Bourtoom, 2007). Yams, cereals, and legumes are the most important sources of starch. Often used as a starch source, yams include sweet potatoes, potatoes, and cassava (Cui, 2005). Starch derived from cassava can be obtained from the meat or the epidermis. Cassava peel starch is often used as an additive in the food and starch-based industries because the starch content is relatively high, namely 44-59% starch (Hui, 2006).

One source of raw materials with biofoam potential is corn because it has 90% cellulose. The availability of cellulose in large quantities will form a strong fiber, insoluble in water, organic solvents, and white (Hauw, 2017). To make it more potent when exposed to water, superhydrophobic properties are needed by adding silica aerogel. Silica aerogels are the only commercially viable ones with excellent overall performance in thermal insulation, stability, and large-scale production (Rao et al., 2006).

## 2. Research Methods

The tools used in this study were beakers, measuring cups, Petri dishes, hot plates, analytical balances, ovens, mortars, spoons, filters, litmus paper, and molds, then the materials used in this study were distilled water, tapioca starch, fiber corn cob, PVA, silica aerogel, NaOH and H<sub>2</sub>O<sub>2</sub>.

### 2.1 Sample Preparation

For corncob fiber, the first step is to dry the corncobs in the sun, then grind them using a blender until they become powder.

### 2.2 Isolation of Cellulose

As much as 50 g of corncob fine powder was soaked with 500 ml of 10% NaOH solution with a solvent ratio (1:10) w/v, stirred using a mixer, and soaked for 24 hours. After that, it is filtered using a filter cloth. The residue obtained is soaked again with 100 ml of solution H<sub>2</sub>O<sub>2</sub> 10% for 24 hours. Then the mixture is filtered, and the resulting residue is washed with distilled water until it smells good H<sub>2</sub>O<sub>2</sub> lost (4 washes). Then the residue was put into the petri dish and in the oven at 50°C for 16 hours.

### 2.3 Manufacture Biofoam

The fine corncob fiber is put into a container, and PVA is added and stirred using a mixer until the dough is fluffy. After that, tapioca starch and silica aerogel were added and stirred using a mixer until the mixture thickened and mixed well. Then the mixture is poured into a mold with a pressure of 100 MPa at a temperature of 70°C for 10 minutes.

**Table 1.** Variation of research samples to be used

Sample	Starch (g)	Fiber (g)	PVA(g)	Silica (g)
A	56.25	13.75	25	15
B	56.25	16.25	25	15
C	56.25	18.75	25	15
D	56.25	21.25	25	15

Variations of starch, fiber, and PVA based on the best biofoam formulation were obtained in a composition of 56.25 g tapioca starch, 18.75 g corn cob fiber, and 25 g PVA (Sumardiono et al., 2021).

### 2.4 Sample Characterization

The characterization is carried out as follows:

1. *Functional Group Analysis.* Functional groups SiO<sub>2</sub> using the iS10 FT-IR Spectrometer at a wavelength range of 4000-300. This analysis is prepared by combining tapioca starch, corncob fiber, PVA, and silica aerogel, then printed using a thermopressing tool to form a flat. The results of this data analysis were carried out by

comparing the results of the wave number table and FT-IR functional groups as well as the results of previous studies.

2. *Crystal Structure Analysis.* Crystal structure characterized using X'Pert Powder PW 30/40 with Cu-K $\alpha$  radiation operated at 40 kV and 30 mA. The characterized sample is flat. The step size is 0.02 per minute in range 2 from 10 to 100°. Qualitative data analysis was performed on QualX software version 2.24, and quantitative analysis was performed on the origin software.

3. *Water Absorption Test.* Testing the water absorption capacity of the sample was carried out by forming a sample in the form of a 2×2 cm pellet. Then, the initial weight of the sample was weighed and immersed in water for 1 minute. The soaked sample is weighed again and recorded as the final weight. The formula lies in Equation (1).

$$DSA (\%) = \frac{m_b - m_k}{m_k} \times 100\% \quad (1)$$

With  $m_k$  is the dry mass (g),  $m_b$  is the mass after soaking for 1 minute (g). The water absorption capacity of the biofoam produced in research (Etikaningrum et al., 2018) is 23.40-45.54%.

4. *Density.* Mass measurement was carried out by weighing the cut biofoam sample with a size of 3×3 cm on an analytical scale. At the same time, volume was calculated by multiplying the length, width, and thickness of the biofoam sample pieces with a vernier caliper. The formula lies in Equation (2).

$$\rho = \frac{m}{V} \quad (2)$$

with  $\rho$  as the density (grams/cm<sup>3</sup>),  $m$  being the mass (grams), and  $V$  as volume (cm<sup>3</sup>). The density value of biofoam produced in research (Etikaningrum et al., 2018) is around 0.16-0.28g/cm<sup>3</sup>.

5. *Compressive Strength Test.* The dimensions of the sample are measured, such as length and width, so that the cross-sectional area stressed on the testing machine can be calculated. Right above the sample is given a load that will press on the middle of the sample. The maximum load value that causes the sample to break or break or break is the material's compressive strength (Ruscahyani, 2020). The formula lies in Equation (3).

$$\sigma = \frac{F_{maks}}{A} \quad (3)$$

with  $\sigma$  as the compressive strength (Mpa),  $F_{maks}$  being the maximum voltage (N), and  $A$  as the surface area (mm<sup>2</sup>).

### 3. Result and Discussion

#### 3.1 Function Group Analysis Result

Functional group analysis of biofoam was carried out to identify the functional groups contained in biofoam at the time of the study. Analysis was performed using FTIR.

The results of the identification of functional groups, such as the **Figure 1** shows that wave number 1157-1026cm<sup>-1</sup> shows peak CO absorption stretching from starch (Coniwanti et al., 2018), at wave numbers 2924-2854cm<sup>-1</sup> showed a stretching CH absorption peak from cellulose material (Singh & Singh, 2013), functional groups at wave numbers 1458-1373cm<sup>-1</sup> shows the bending CH absorption peaks of PVA (Wijaya et al., 2022), and functional groups at wave numbers 933-918cm<sup>-1</sup> showed absorption peaks of SiO from silica (Görlich, 1982).

Along with increasing the amount of fiber, there are some changes, such as differences in value transmittance. Wave number 2924-2854 cm<sup>-1</sup> with a transmittance value of 22.00-7.29% characterizes the CH functional group (Hanjitsuwan et al., 2011) has a lower transmittance value than wave number 933-918 cm<sup>-1</sup> with a transmittance value of 30.08-11.71% which characterizes the SiO functional group. It indicates the effect of the number of fibers on the transmittance value (Coates, 2000). In addition, the functional groups OH and C=C were obtained in biofoam. It indicated that lignin was still due to the poor bleaching when isolating cellulose from corn cobs (Aditama & Ardhyanta, 2017).

Functional group identification results are shown in **Table 2** The results in **Figure 1** show the spectrum of the OH functional group having sharper areas than the other functional groups. It is because FTIR spectrophotometry works based on interactions or relationships on the vibrations of molecular atoms, which bond to each other with the OH functional groups in molecules by absorbing radiation in IR electromagnetic waves. The absorption process of FTIR radiation can cause an increase in the energy of molecular vibrations to a higher vibrational level, and the magnitude of this absorption can be specific and even better (Sulistiyani & Huda, 2017).

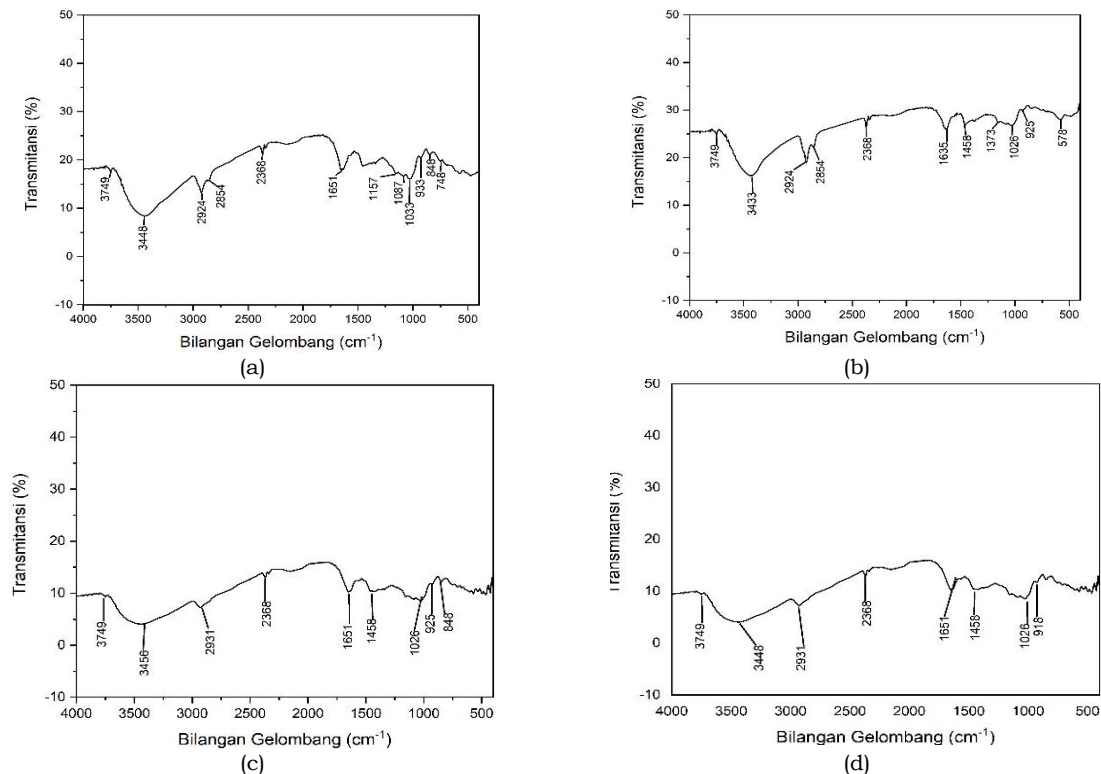


**Figure 1.** The results of identification of functional groups in the biofoam sample (a) Sample A, (b) Sample B, (c) Sample C, (d) Sample D.

**Table 2.** Cluster Identification Result.

Wave Number (cm <sup>-1</sup> )				Group Functions	Score Transmittan (%)	Type Vibration	Reference
Sample A	Sample B	Sample C	Sample D				
3749-3448	3749-3433	3749-3456	3749-3448	O-H	25.08-4.06	stretching	Kizil dkk (2002)
2924-2854	2924-2854	2931	2931	C-H	22.01-7.29	stretching	Singh & Singh (2013)
1651	1635	1651	1651	C=C	26.10-10.26	stretching	Singh & Singh (2013)
1157-1033	1026	1026	1026	C-O	26.86-8.54	stretching	(Coniwanti dkk, 2018)
-	1458-1373	1458	1458	C-H	27.40-10.38	bending	Wijaya dkk, 2022)
933	925	925	918	SiO	30.08-11.71	systematic bending	(Görlich, 1982)
848	-	848	-	C-H	21.26-12.17	deformation	Zghari dkk (2018)
748	-	-	-	C-H	19.84	bending	Zghari dkk (2018)

### 3.2. Crystal Phase

Analysis of the crystal structure of the biofoam material was carried out to determine the phase and crystal structure using the QualX software (Altomare et al., 2015). In Qualx, no cellulose phase was found, so a literature study was carried out referring to the article by Nishiyama et al. (2002). This method is carried out by matching the experimental data with the crystallographic database (COD). The data obtained is the relationship between the intensity and the angle two theta ( $2\theta$ ) value presented as a diffractogram. In the diffractogram, there is the highest peak can be known using the Rietica software.

Based on the results of matching the experimental data with the COD database, crystals cellulose which has a monoclinic structure with a space group P 1 1 21 according to the results of research from (nisyama, 2002) where the value  $a$  (Å)=8.01,  $b$  (Å)=9.04,  $c$  (Å)=10.36,  $\gamma$  (Å)=117.1 and  $Z=2$ . Then on phase, silica has an Orthorhombic structure with space group I c m a, where for the value  $a$  (Å)=4.7200,  $b$  (Å)=5.1600,  $c$  (Å)=8.3600,

and  $Z=4$ . It means that biofoam only has 2 phases, each with the highest peak.

Phase silica (COD 00-810-4322) is at a value of 2 as big  $21.84^\circ$  with a Miller index (101), and phase cellulose (COD 41-14-994) also appears on two as big  $21.14^\circ$  with a Miller index (102). The diffractogram of this matching result is shown in **Figure 2**. phase appears, silica and cellulose agreed with the FTIR results, which confirmed the functional group bonds between CH and Si-O. XRD data were refined using the Rietveld method and Rietica software to determine each phase's composition.

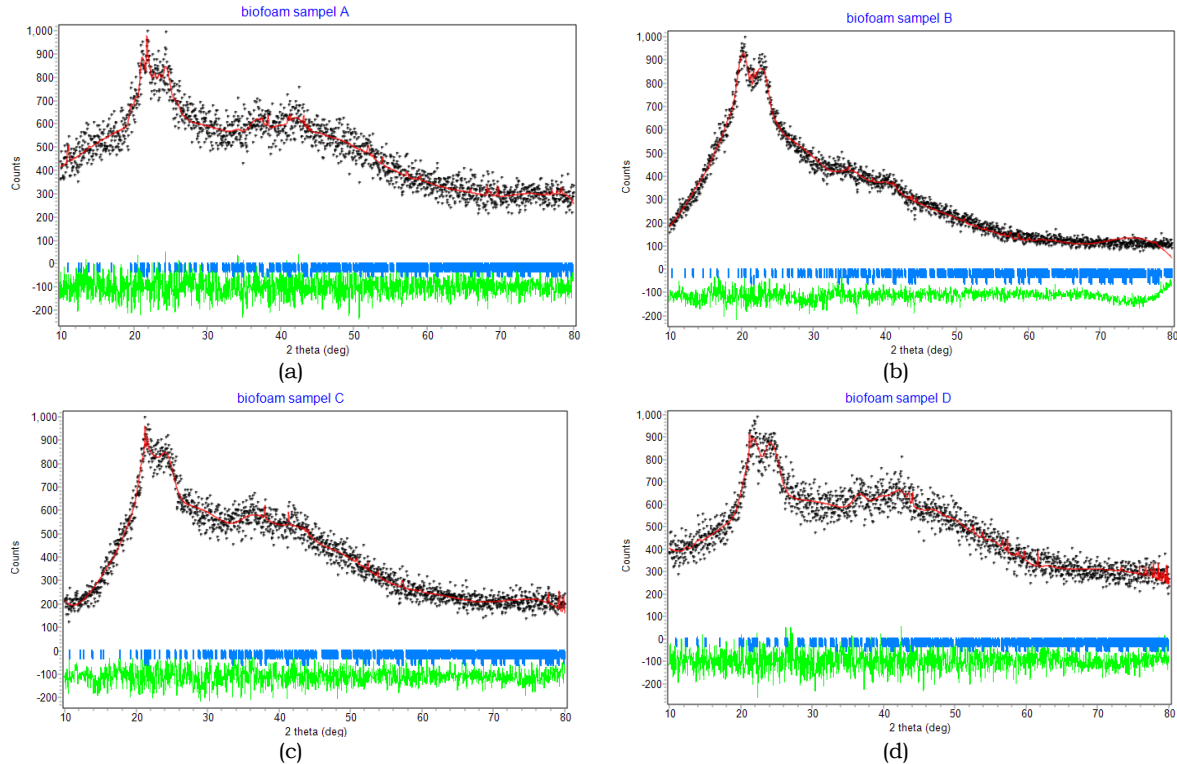


**Figure 2.** Results refinement XRD data sample A, B, C, and D.

The analysis of quantitative data is shown in **Figure 2**. The starch and PVA phases were not detected because they have a semi-crystalline structure. In starch and PVA, intermolecular van der Waals bonds are caused by an asymmetrical charge distribution.

Then the results of the quantitative analysis were followed by a quantitative analysis with the suitability parameters and phase percentage shown in **Table 3**, **Table 4**, and **Table 5**.

**Table 3.** Percentage of parameters for refinement of XRD data biofoam.

Sample	$R_{WP}$	$R_p$	$R_{exp}$	$G_oF$
A	8.10	6.84	5.01	0.26
B	5.44	5.66	5.93	0.84
C	7.27	6.32	6.02	0.14
D	7.92	6.41	5.20	0.23

In the refinement results, the XRD data parameters are obtained as follows in **Table 3**, where the refinement results for all samples show  $R_{exp}$ ,  $R_{wp}$ , and  $R_p$ , values of less than 9%, and Goodness of Fit ( $GoF$ ) values of less than 1%. Less than 9% and  $GoF$  less than 1%. The percentage value of  $GoF$  is less than 4%, and  $R_{wp}$  is less than 25% (Kisi, 1994). Furthermore, the refined data is used to determine the molar percentage of each phase and the percentage of the phase in percent by weight (%wt) obtained from qualitative data. The results of the molar percentage of each phase and the percentage of the phase in percent by weight (% wt) can be seen in **Table 4** and **Table 5**.

**Table 4.** Percentage of molar phase in the sample (%).

Sample	Cellulose (%)	Silica (%)
A	62.48	37.52
B	63.71	36.29
C	61.21	38.79
D	61.95	38.05

**Table 5.** Phase percentage in weight percent (% wt).

Phase Type	A	B	C	D
Celulose	89.99232	90.45814	89.49703	89.78743
Silica	10.02161	9.555143	10.51759	10.22678
Total	100	100	100	100

**Table 4** and **Table 5** show that each phase's composition changes significantly with the amount of fiber. **Table 4** shows that the percentage of cellulose phase was 62% and decreased, which was insignificant as the amount of fiber increased. It is inversely proportional to the percentage of silica phase, which is 37%, and increases with fiber content. Next, **Table 5** showed that the phase composition did not change significantly with the amount of fiber. The cellulose phase was 89% (% wt) and decreased as the amount of fiber increased. It has the opposite effect with the percentage of silica phase, which is in the range of 10% (%wt) and increases with the number of fibers.

Then adding the number of fibers causes a change in the cell parameters of each current phase. The following cell parameters of each phase are shown in **Table 6**, **Table 7**, and **Table 8**.

**Table 6.** Cellulose Parameters.

Sample	$a$ (Å)	$b$ (Å)	$c$ (Å)	$\alpha$ (°)	$\beta$ (°)	$\gamma$ (°)
A	7.89	9.22	10.61	90.00	90.00	117.47
B	7.72	9.76	10.60	90.00	90.00	118.63
C	7.95	9.25	10.40	90.00	90.00	117.38
D	7.96	9.03	10.36	90.00	90.00	116.98

**Table 7.** Silica Parameter.

Sample	$a$ (Å)	$b$ (Å)	$c$ (Å)	$\alpha$ (°)	$\beta$ (°)	$\gamma$ (°)
A	4.73	5.18	8.41	90.00	90.00	90.00
B	4.70	5.16	8.36	90.00	90.00	90.00
C	4.72	5.16	8.36	90.00	90.00	90.00
D	4.72	5.16	8.36	90.00	90.00	90.00

**Table 8.** Parameters of silica cells with added fiber.

Sample	Cellulose	Silica
A	206.54	206.54
B	202.92	202.92
C	203.83	203.83
D	203.60	203.60

Based on the results of phase analysis in **Table 6**, **Table 7**, and **Table 8** shows the size of the cell parameters of the four phases, it can be seen that each phase experienced an increase and decrease even though it did not occur significantly, but this increase and decrease caused changes in the unit cell volume in the phase structure.

### 3.3 Water Absorption

The water absorption test aims to determine the amount of water content that can be absorbed by biofoam, which has been added with silica aerogel. Determination of the water absorption capacity of biofoam can be obtained from the measurement results of dry mass and wet mass, each of which is measured using an analytical balance. The sample was measured to be 2×2 cm and then immersed in water for 1 minute to obtain the final weight.

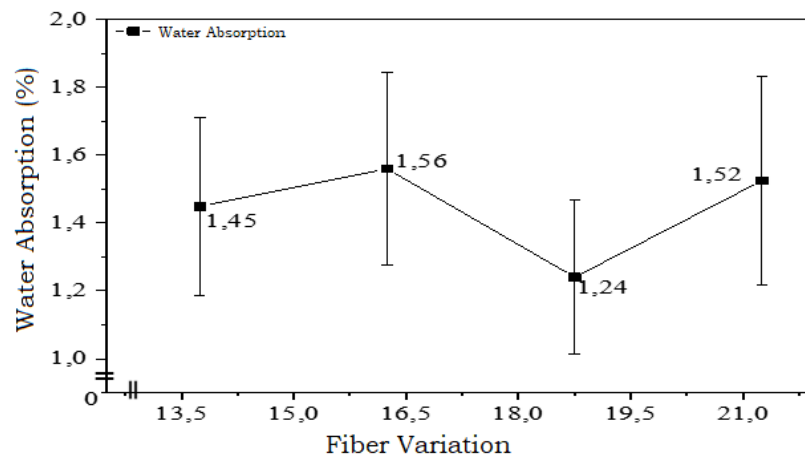


**Figure 3.** Water Absorption Test Results in Biofoam.

The graph is shown in **Figure 3** results from the water absorption value calculated using Equation (1). The results of the water absorption test show nonlinearity. It follows the research conducted by Iriani (2013) that the more fiber, the greater the water absorption capacity obtained. In contrast, absorbing water is more significant in this fiber variation because fiber has hydrophilic properties, which means it is like water. This study increases the value of water absorption (Solechudin & Wibisino, 2002).

This study's best water absorption analysis was  $(1.2 \pm 0.23)\%$ . It is different from research conducted by Etikaningrum et al. (2018). In the research by Etikaningrum et al. (2018), a water absorption capacity of 23.40-45.54% was obtained. The difference in the results obtained is due to the different fiber types.

### 3.4 Density

Density testing aims to determine the mass and volume of the biofoam sample, the sample is measured to be  $3 \times 3$  cm, and the mass and volume are measured using an analytical balance and digital calipers.

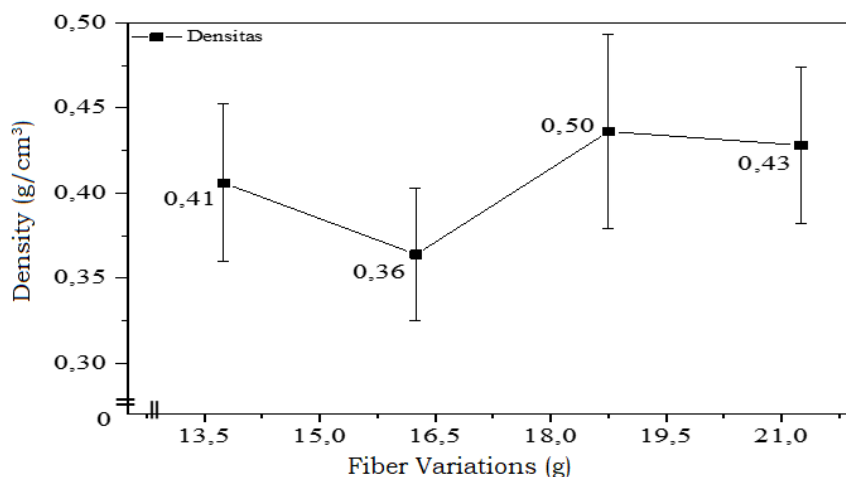


**Figure 4.** Density Calculation Results.

The graph shown in **Figure 4** is the density value calculated using Equation (2). The results of the density test show nonlinearity. In the process of making biofoam, the expansion process that occurs will produce biofoam with a hollow structure. However, if the dough is added with cellulose fiber, the cavity formed will shrink due to the inhibition of the expansion process. The inhibition of the expansion process results in a denser biofoam with a high density. In addition, the disruption of the expansion process will have an impact on decreasing the porosity of the biofoam and increasing the density of the resulting biofoam. Adding this fiber can also fill the empty spaces in the starch (matrix), thereby increasing the density of biofoam (Ritonga, 2019).

The density analysis obtained in this study was  $(0.5 \pm 0.1) \text{ g/cm}^3$  when compared with research conducted by Etikaningrum et al. (2018), a density of 0.16-0.28  $\text{g/cm}^3$  was obtained. The difference in results obtained by insulating other cellulose and the type of fiber used is also different.

### 3.5 Compressive Strength

The compressive strength test on biofoam aims to determine the strength of biofoam in protecting products packaged in biofoam. Biofoam with a high compressive strength value is expected to be environmentally friendly packaging with properties that are not easily damaged and broken and can survive to maintain the shape of the packaging (Iriani, 2013).

The compressive strength test shows nonlinearity. The graph shown in **Figure 5** is the compressive strength value calculated. The compressive strength results tend to decrease in the four samples due to an increase in the density value, which affects the compressive strength of biofoam, following the density results in **Figure 5**, where the increase in the density value significantly affects the compressive strength, which results in a decrease in the compressive strength value that occurs in the number of fibers of 21.25g with a compressive strength value of 0.99Mpa. This value is smaller compared to previous research conducted by Sumardiono et al. (2021), which is 14.16Mpa. It follows the statement of Hu et al. (2015) that the addition of too much fiber can cause a decrease in its physical properties, making biofoam break quickly.

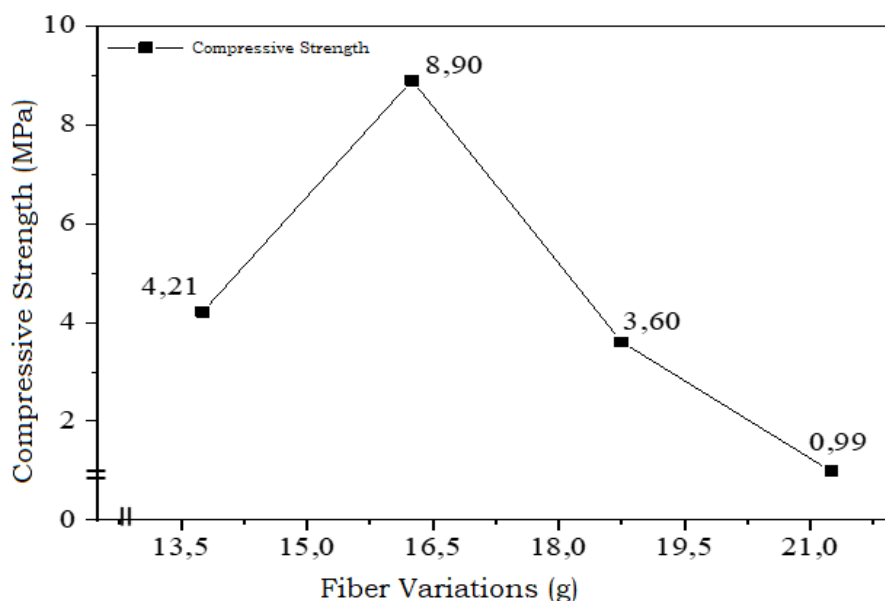


**Figure 5.** Compressive Strength Calculation Results.

#### 4. Conclusions

This study showed that biofoam from starch, fiber, PVA, and silica showed CH and SiO bonds in FTIR, indicating the formation of cellulose and silica phases from the results of XRD characterization. Furthermore, in the range of phase molar percentages, weight, and unit cell volume percentages decreased, which was not significant, followed by physical tests, which showed nonlinearity affected by increasing the number of fibers. The results obtained from each biofoam test with the addition of corn cob concentrations (13.75g, 16.25g, 18.75g, and 21.25g), respectively, were the water absorption test of  $1.45 \pm 0.26\%$ ,  $1.56 \pm 0.24\%$ ,  $1.24 \pm 0.23\%$ , and  $1.52 \pm 0.32\%$ , density  $0.41 \pm 0.05\text{g/cm}^3$ ,  $0.36 \pm 0.04\text{g/cm}^3$ ,  $0.0$ ,  $50 \pm 0.06\text{g/cm}^3$  and  $0.43 \pm 0.05\text{g/cm}^3$ , and compressive strengths of 4.21MPa, 8.90MPa, 3.60MPa, and 0.099MPa.

#### 5. References

- Aditama, A. G. & Ardhyanta, H. (2017). Isolasi Selulosa dari Serat Tandan Kosong Kelapa Sawit untuk Nano Filler Komposit Absorpsi Suara: Analisis FTIR. *Jurnal Teknik ITS*. Vol. 6. No. 2. Hal. 228–231.
- Altomare, A., Corriero, N., Cuocci, C., Falcicchio, A., Moliterni, A., & Rizzi, R. (2015). Qualx2.0: A Qualitative Phase Analysis Software using The Freely Available Database POW-COD. *Journal of Applied Crystallography*. Vol. 48. No. 1. Pg. 598–603.
- Bourtoom, T. (2007). Effect of Some Process Parameters on The Properties of Edible Film Prepared from Starches. *Department of Material Product Technology*. Vol. 51. No. 2. Pg. 61–73.
- Breuninger, W. F., Piyachomkwan, K., & Sriroth, K. (2009). *Tapioca/Cassava Starch: Production and Use, Bemiller, Starch: Chemistry and Technology*. Elvieser Inc.
- Coates, J. (2000). *Interpretation of Infrared Spectra, A Practical Approach*. R.A. Meyers.
- Coniwanti, Roosdiana, P., & Mu'in. (2018). Pengaruh Konsentrasi NaOH Serta Rasio Serat Daun Nanas dan Ampas Tebu Pada Pembuatan Biofoam. *Jurnal Teknik Kimia*. Vol. 24. No. 1. Hal. 1–7.
- Cui, S. (2005). *Food Carbohydrates Chemistry, Physical Properties, and Applications*. CRC Press. Boca Raton.
- Cullity, B. (1977). *Element of X-Ray Diffraction second edition*. Addison Wesley Publishing Company.
- Debiagi, F., Mali, S., Grossmann, M. V. E., & Yamashita, F. (2011). Biodegradable Foams Based on Starch, Polyvinyl Alcohol, Chitosan and Sugarcane Fibers Obtained by Extrusion. *Brazilian Archives of Biology and Technology*. Vol. 54. No. 5. Pg. 1043–1052.
- Etikaningrum, N., Hermanianto, J., Iriani, E. S., Syarif, R., & Permana, A. W. (2018). Pengaruh Penambahan Berbagai Modifikasi Serat Tandan Kosong Sawit Pada Sifat Fungsional Biodegradable Foam. *Jurnal Penelitian Pascapanen Pertanian*. Vol. 13. No. 3. Hal. 146-155.



- Görlich, E. (1982). The structure of SiO<sub>2</sub> - Current views. *Ceramics International*. Vol. 8. No. 1. Pg. 3–16.
- Hanjitsuwan, S., Chindaprasit, P., & Pimraksa, K. (2011). Electrical Conductivity and Dielectric Property of Fly Ash Geopolymer Pastes. *International Journal of Minerals, Metallurgy, and Materials*. Vol. 1. No.18. Pg. 94-99.
- Hauw, A. (2017). Pengaruh Pretreatment Inokulum EM4, Suhu, Waktu Dan Tekanan Terhadap Fermentasi Kelobot Jagung (*Zea Mays L.*). *Skripsi*. Universitas Atma Jaya.
- Hu, F., Lin, N., Chang, P., & Huang, J. (2015). Reinforcement and Nucleation of Acetylated Cellulose Nanocrystal Infoamed Polyester Composites. *Carbohydrate Polymers*. Vol. 129. No. 1. Pg. 208–215.
- Hui, Y. H. (2006). *Handbook of Food Science, Technology, and, Engineering*. CRC Press.
- Iriani, E. (2013). Pengembangan Produk Biodegradable Foam Berbahan Baku Campuran Tapioka dan Ampok. *Skripsi*. Institut Pertanian Bogor.
- Kaisangsri, N., Kerdchoechuen, O., & Laohakunjit, N. (2014). Characterization of Cassava Based Foam Blended with Plant Proteins, Kraft Fiber, and Palm Oil. *Carbohydrate Polymers*. Vol. 110. No. 1. Pg. 70–77.
- Khalid, K., Moorthy, R., & Saad, S. (2012). Environmental Ethenies in Governing Recycled Material Styrofoam for Building Human Habitat. *American Journal Environmental Science*. Vol. 8. No. 6. Pg. 591–596.
- Kizil, R., Irudayaraj, J., & Seetharaman, K. (2002). Characterization of Irradiated Starches by Using FT-Raman and FTIR Spectroscopy. *Journal of Agricultural and Food Chemistry*. Vol. 50. No. 14. Pg. 3912–3918.
- Nishiyama, Y., Langan, P., & Chanzy, H. (2002). Struktur Kritis dan Sistem Ikatan Hidrogen dalam Selulosa dari Sinar -X Synchrotron dan Difraksi Serat Newton. *Jacs Articles*. 38041.
- Qiu, J., Zhang, M., Rong, M., Wu, S., & Karger-korcis, J. (2013). Rigid Bio-Foam Plastics with Intrinsic Flame Retardancy Derived from Soybean Oil. *Journal of Material Chemistry*. Vol. 1. Pg. 2533–2542.
- Rao, A. P., Rao, A. V., & M, P. G. (2006). Hydrophobic and Physical Properties of The Ambient Pressure Dried Silica Aerogel with Sodium Silicate Precursor Using Various Sililating Agents. *Applied Surface Science*. Vol. 253. No. 17. Pg. 6032–6040.
- Ruscahyani, Y., Oktorina, S., & Hakim, A. (2021). Pemanfaatan Kulit Jagung Sebagai Bahan Pembuatan Biodegradable Foam. *Jurnal Teknologi Technoscientia*. Vol. 14. No. 1. Hal. 25–30.
- Singh, R. K., & Singh, A. K. (2013). Optimization of Reaction Conditions for Preparing Carboxymethyl Cellulose from Corn Cob Agricultural Waste. *Waste and Biomass Valorization*. Vol. 4. No. 1. Pg. 129–137.
- Sulchan, M., & Endang, N. (2007). Keamanan Pangan Kemasan Plastik dan Styrofoam. *Majalah Kedokteran Indonesia*. Vol. 57. No. 2. Hal. 54–59.
- Sulistiyani, M., & Huda, N. (2017). Optimasi Pengukuran Spektrum Vibrasi Sampel Protein Menggunakan Spektrofotometer *Fourier Transform Infra Red* (FTIR). *Indonesian Journal of Chemical Science*. Vol 6. No. 2. Hal. 173–180.
- Sumardiono, S., Pudjiastuti, I., & Amalia, R. (2021). Kajian Sifat Morfologo dan Mekanis Biofoam dari Tepung Tapioka dan Serat Limbah Batang Jagung. *Metana: Media Komunikasi Rekayasa Proses dan Teknologi Tepat Guna*. Vol. 17. No. 1. Hal. 22–26.
- Wijaya, G. H., Sutiarno, S., Karokaro, P., Syafriadi, S., Ginting, P., & Riyanto, A. (2022). Pengaruh Variasi Ion Ag<sup>+</sup> terhadap Pembentukan Biofoam Antibakteri Berbasis Pati Singkong dan Selulosa Batang Jagung. *Journal Phi*. Vol. 3. No. 2. Hal. 49–61.
- Zghari, B., Hajji, L., & Boukir, A. (2018). Effect of Moist and Dry Heat Weathering Conditions on Cellulose Degradation of Historical Manuscripts Exposed to Accelerated Ageing: C NMR and FTIR Spectroscopy as a Non-Invasive Monitoring Approach. *Journal of Materials and Environmental Science*. Vol. 9. No. 2. Pg. 641–654.